Effect of close coupling on performance of a modal filter with the passive conductor in the reference plane cutout

Effect of close coupling on performance of a modal filter with the passive conductor in the reference plane cutout

M A Samoylichenko and T R Gazizov

Tomsk State University of Control Systems and Radioelectronics, 40, Lenina ave., Tomsk, 634050, Russia

E-mail: 1993mary2011@mail.ru

Abstract. The improvement of protection against an ultrashort pulse (USP) using a modal filter with the passive conductor implemented in the reference plane cutout is considered. The influence of segmentation on the simulation results is shown. The effect of close coupling on the difference between mode delays and the amplitudes of decomposition pulses was studied. Minimization and alignment of the pulse amplitudes are achieved. The possibility of increasing USP attenuation to 5 times for a given material is shown.

1. Introduction

Ensuring the electromagnetic compatibility of electronic equipment (EE) is one of the urgent problems since the creation of new EE and modernization of the existing one, as well as the rapid increase in the number of simultaneously operating EE, lead to appearance of inductive and conductive electromagnetic interference. One of the threats is a powerful ultrashort pulse (USP), which leads to equipment failure, accidents and malfunctions [1]. Therefore, protection against USP is relevant.

A new means for protecting equipment against USP is a modal filter (MF) [2-6]. The main idea of the MF is to decompose the USP into pulses of lower amplitude due to different per-unit-length delays of the T-wave modes in a coupled line with a nonhomogeneous dielectric filling. In the previous studies, MFs have been realized with a passive conductor, which takes up additional space and complicates the implementation of modal filtering in printed circuit boards. Therefore, it is important to explore new approaches to MF morphology.

Thus, it was proposed to place the passive conductor in the cutout of a reference plane. The paper [7] shows the input pulse attenuation of 2.94 times and it is believed that greater attenuation can be achieved by increasing the coupling between the active and passive conductors. The purpose of the work is to carry out such study.

2. Description of MF

The technology of modal filtering is based on a microstrip line. In the reference plane of the line there are two cutouts that form a passive conductor. Figure 1 shows the MF cross section, where ε_r is the relative permittivity of the substrate, w_1, w_2, w_3 are the widths of the conductors, t is the thickness of the conductors, h is the substrate thickness, s is the separation of the conductors. Foil-clad fiberglass (ε_r = 4.5) was chosen as the substrate material because of its low cost, availability and widespread use.

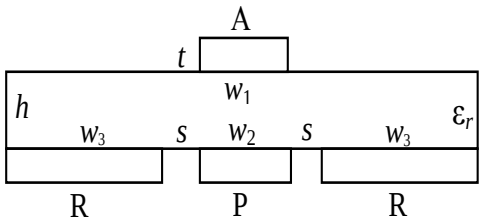

Figure 1. MF cross section, where the conductors: R – reference, A – active, P – passive.

The MF connection diagram is shown in Figure 2*a*. The active conductor is connected to a pulse signal source, represented in the circuit as an ideal e.m.f. source *E* and internal resistance *R*1. The other end of the active conductor is connected to load *R*4. The resistance values *R*1, *R*2, *R*4, *R*5 are assumed to be the same and equal to 50 Ω, and *R*3 = *R*6 = 0.001 Ω for connecting the side conductors. The input excitation is a trapezoidal pulse, shown in Figure 2*b*, with parameters: an e.m.f. amplitude of 2 V, rise time of 150 ps, flat peak time of 200 ps, fall time of 150 ps. The calculation of parameters and waveforms has been performed using the quasistatic approach in the TALGAT system [8]. Losses in conductors and dielectrics were not taken into account.

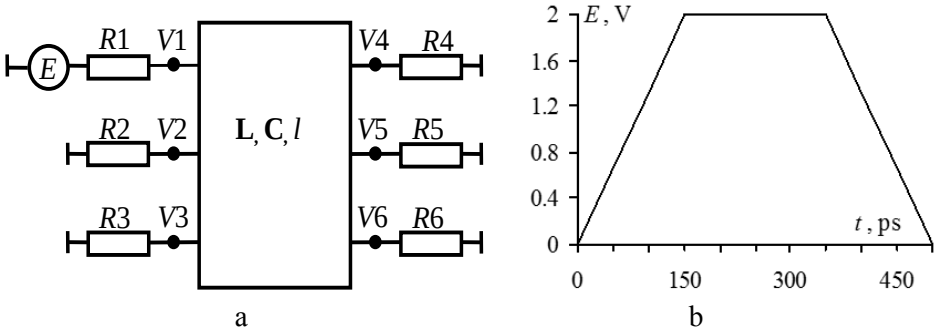

Figure 2. MF connection diagram (*a*) and exciting EMF waveform (*b*).

3. Simulation results

The simulation was performed with typical parameters of foil-clad fiberglass: t = 35 μm, h = 0.18 mm with an MF length (l) of 30 cm. Since the material parameters are fixed, to increase the coupling we simultaneously increased only the width of the active (w_1) and passive (w_2) conductors ($w_1 = w_2$) from 1 to 3.5 mm (in 0.1 mm increments) and gaps (s) from 0.5 to 3.5 mm (in 0.2 mm increments). The width of the side conductors did not change (w_3 = 0.5 mm). The optimization was performed according to the criteria of minimizing the amplitude output voltage and maximizing the difference in the mode delays.

Rare segmentation and asymmetry of matrices **L** and **C** lead to incorrect results. Therefore, we performed preliminary simulation with increased segmentation. It was taken uniform at all boundaries, but was controlled by the number of segments (n) at conductor edges (from 1 to 7). Its effect on matrix asymmetry and mode delays was estimated and the absence of significant changes in the results indicated their convergence. We simulated the case of maximum coupling between the passive and active conductors ($w_1 = w_2$ = 3.5 mm, w_3 = 0.5 mm, s = 3.5 mm).

The entries of the original (asymmetric) matrices **L** and **C** are given in Table 1, and symmetrized (by arithmetic mean.value) – in Table 2. The maximum entries of the asymmetry matrices are summarized in Table 3. Elements of asymmetry matrices were calculated as:

$$(|X_A - X_S| / (X_S|)\cdot 100\% \quad (1)$$

where, X_A is the entry of the asymmetric matrix, X_S is the symmetrized elements of the entry original matrix.

The analysis of Table 1 does not show unphysical results (off-diagonal entry elements of matrix **C** are negative even with the rarest segmentation). However Table 3 shows a rather large asymmetry of

matrix **C** (more than 40%) with $n = 1$. This means that these results may be incorrect. Meanwhile, when increasing segmentation, the asymmetry decreases to 2% with $n = 3$, so now the results are applicable for further calculations.

Table 1. Original Matrices

n	Matrices					
	L, nH/m			C, pF/m		
1	1.06237	1.03296	8.42981	8.10909	–8.03958	–8.09548
	1.03296	1.06207	8.42981	–8.0399	8.10868	–8.19332
	8.44739	8.44739	1.68948	–3.45544	–3.45502	1.6057
3	1.06222	1.03284	8.43127	8.1345	–8.02376	–5.30873
	1.03284	1.06192	8.43127	–8.02371	8.13493	–5.32213
	8.43879	8.43879	1.68776	–5.54232	–5.55874	1.32571
5	1.06242	1.03304	8.4342	8.13338	–8.02451	–5.42828
	1.03304	1.06213	8.4342	–8.0245	8.13373	–5.44593
	8.43727	8.43727	1.68745	–5.44386	–5.46115	1.33676
7	1.0626	1.03322	8.43654	8.13476	–8.02595	–5.44064
	1.03322	1.0623	8.43654	–8.02594	8.13511	–5.45824
	8.43654	8.43654	1.68731	–5.44082	–5.45806	1.33817

Table 2. Symmetrized Matrices

n	Matrices					
	L, Hn/m			C, F/m		
1	1.06237	1.03296	8.4386	8.10909	–8.03978	–5.77546
	1.03296	1.06207	8.4386	–8.03978	8.10868	–5.82417
	8.4386	8.4386	1.68948	–5.77546	–5.82417	1.6057
3	1.06222	1.03284	8.43503	8.13456	–8.02373	–5.42552
	1.03284	1.06192	8.43503	–8.02373	8.13493	–5.44043
	8.43503	8.43503	1.68776	–5.42552	–5.44043	1.32571
5	1.06242	1.03304	8.43574	8.13338	–8.02451	–5.43607
	1.03304	1.06213	8.43574	–8.02451	8.13373	–5.4535
	8.43574	8.43574	1.68745	–5.43607	–5.45354	1.33676
7	1.0626	1.03322	8.43654	8.13476	–8.02595	–5.44073
	1.03322	1.0623	8.43654	–8.02595	8.13511	–5.45815
	8.43654	8.43654	1.68731	–5.44073	–5.45815	1.33817

Table 3. Maximum values of asymmetry matrix entries

n	Values, %	
	L	C
1	0.104	40.678
3	0.045	2.175
5	0.018	0.143
7	$1.4 \cdot 10^{-7}$	0.002

The per-unit-length delays and mode arrival times, calculated from symmetrized matrices **L** and **C**, are given in Table 4. It is seen that for $n = 1$ $\tau_1 = 2.37451$ ns/m, which is physically impossible, since the delays should be no less than 3.3 ns/m, in accordance with the speed of light in vacuum. When increasing segmentation, the accuracy increases: the values of τ for $n = 3$ and $n = 5$ coincide to one decimal place. This is sometimes acceptable, but in this case of close values of τ_1 and τ_2, higher accuracy is desirable.

The values of τ for $n = 5$ and $n = 7$ segments coincide up to three decimal places. This makes it possible to use $n = 5$ in further simulations to save time. An example of calculating the time response for $n = 5$ is shown in Figure 3. The first two fast modes arrive approximately simultaneously and in

accordance with the values (≈1 ns) given in Table 4. They are presented as a single pulse, since the difference in mode delays is very small (0.01 ns). The third mode also corresponds to the value from Table 4 (≈2 ns).

Table 4. Per-unit-length delays and mode arrival times

n	**τ_1, ns/m**	**τ_2, ns/m**	**τ_3, ns/m**	**$\tau_1 \cdot l$, ns**	**$\tau_2 \cdot l$, ns**	**$\tau_3 \cdot l$, ns**
1	2.37451	4.04863	6.87312	0,712353	1,214589	2,061936
3	3.64804	3.7405	6.87293	1,094412	1,12215	2,061879
5	3.6581	3.69495	6.87244	1,09743	1,108485	2,061732
7	3.65844	3.69399	6.87285	1,097532	1,108197	2,061855

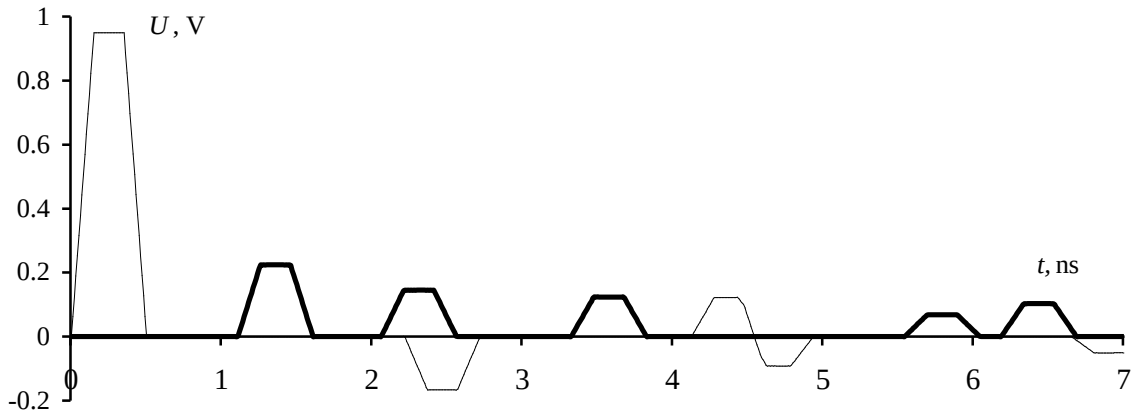

Figure 3. Voltage waveforms at the beginning (-) and end (-) of the MF active conductor.

The dependences of τ on w_1 for different s are shown in Figure 4. The values of τ, in spite of the increase in the coupling, do not change significantly. This is due to the fact that both fast modes almost completely propagate in air, and the slow one – in the dielectric.

For all values of w_1 and s, the voltage waveforms were calculated similarly to Figure 4. They showed that the output voltage amplitude is determined by the varying amplitudes of the first two pulses. Their dependences on w_1 for different values of s are shown in Figure 5.

The amplitude of the first pulse depends weakly on w_1, but decreases with increasing s from about 0.3 V to 0.2 V. The amplitude of the second pulse decreases with increasing w_1 from about 0.35 V to 0.15 V, but does not depend much on s. As a result, the graphs intersect at a point corresponding to the equality of the pulse amplitudes, which decrease to 0.21 V with the increase in s to 3.5 mm at w_1 = 2.1 mm. The voltage waveforms for this case are shown in Figure 6.

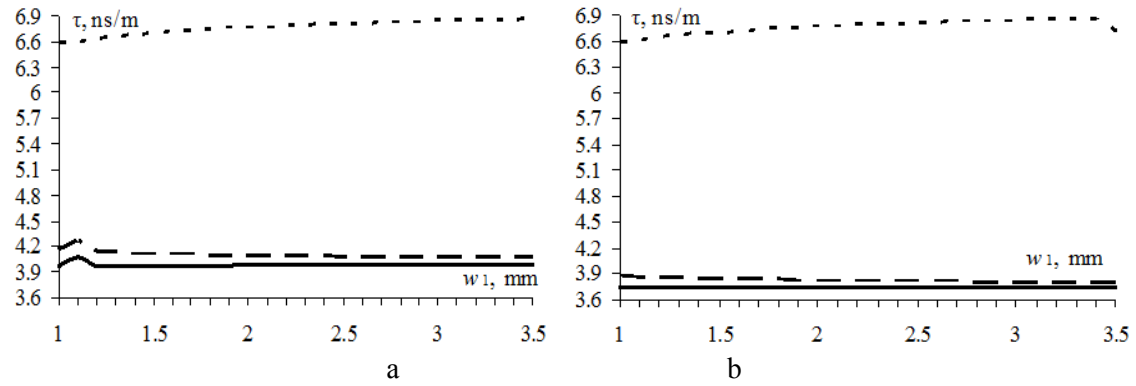

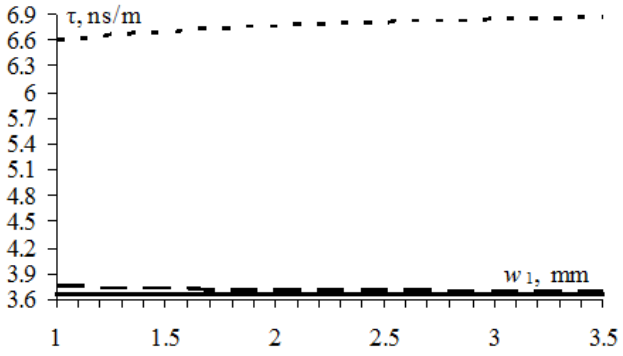

c

Figure 4. Dependences of τ_1 (—), τ_2 (--), τ_3 (----) on w_1 for s=0.7 (a), 1.9 (b), 3.5 (c).

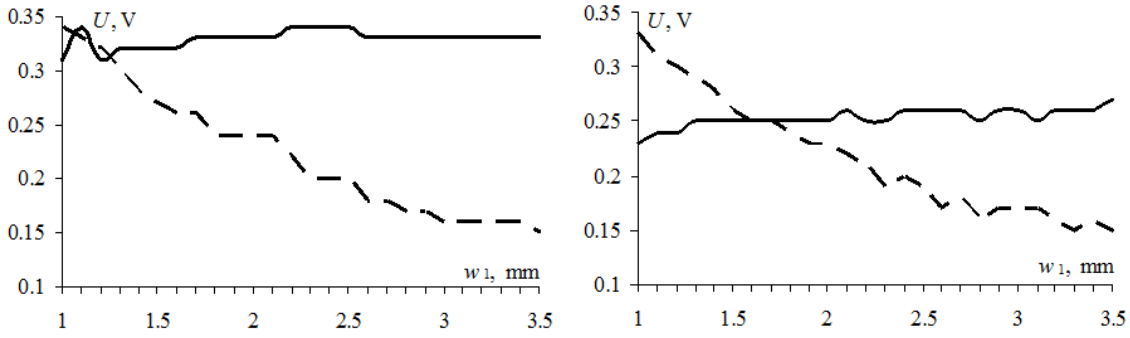

a b

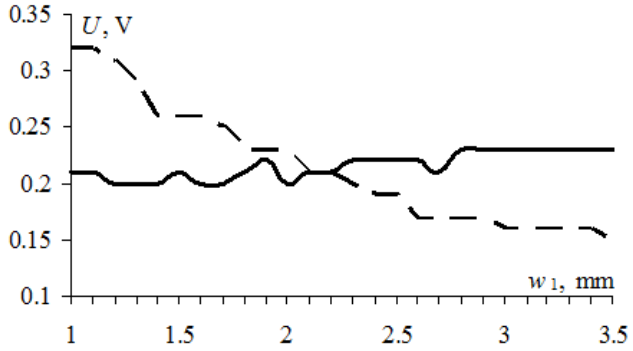

c

Figure 5. Dependences of U_2 (—) and U_3 (--) on w_1 for s=0.7 (a), 1.9 (b), 3.5 (c).

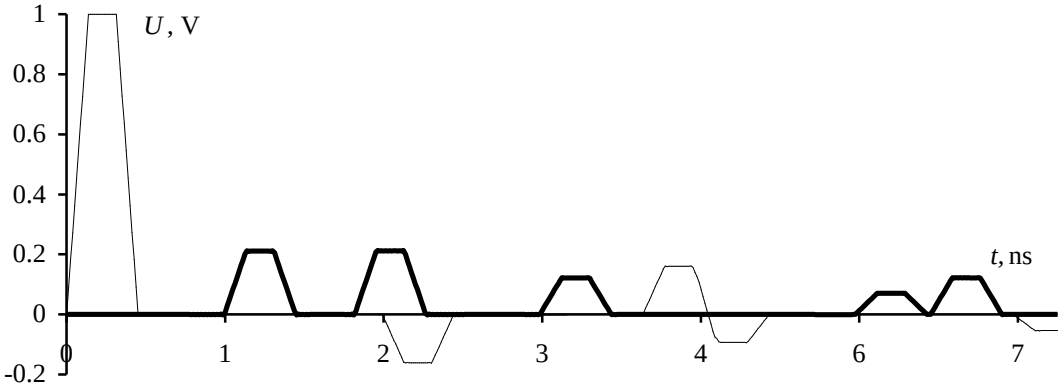

Figure 6. Voltage waveforms at the beginning (-) and end (-) of the MF active conductor.

4. Conclusion

Thus, it is shown that for a given material for an MF, by increasing the coupling between the active and passive conductors, it is possible to achieve 5-time attenuation of a USP with respect to half the e.m.f., while the duration of the USP to be decomposed can be increased to 1 ns. In future there will be a study of the influence of the boundary conditions at the ends of the passive conductor, which will allow for greater attenuation.

5. Acknowledgments

The reported study was supported by the Ministry of Science and Higher Education of the Russian Federation (Project 8.9562.2017/8.9).

References

[1] Gizatullin Z M and Gizatullin R M 2016 *Journal of Communications Technology and Electronics* **5** 546–550
[2] Khazhibekov R and Zabolotsky A M 2019 *Int. Siberian Conf. on Control and Communications (SIBCON 2019)* pp 1–4
[3] Chernikova E, Belousov A and Zabolotsky A M 2019 *Int. Siberian Conf. on Control and Communications (SIBCON 2019)* pp 1–4
[4] Belousov A, Zabolotsky A M and Gazizov T T 2017 *18th Int. Conf. of Young Specialists on Micro/Nanotechnologies and Electron Devices EDM* pp 46–49
[5] Khazhibekov R, Zabolotsky A M and Khramtsov M V 2017 *Proc. of IEEE 2017 Int. multi-conf. on engineering, computer and information science* pp 506–509
[6] Gazizov A T, Zabolotsky A M and Gazizov T T 2016 *17th Int. Conf. of Young Specialists on Micro/Nanotechnologies and Electron Devices* pp 85–88
[7] Samoylichenko M A and Gazizov T R 2019 *Journal of physics: conference series* 1–7
[8] Kuksenko S P, Gazizov T R, Zabolotsky A M, Ahunov R R, Surovtsev R S, Salov V K and Lezhnin Eg V 2015 *Advances in Intelligent Systems Research (ISSN 1951-6851). Proc. of the 2015 Int. Conf. on Modelling, Simulation and Applied Mathematics (MSAM2015)*